ICARUS 83, 308–324 (1990)

Titan's Thermosphere Profile

EMMANUEL LELLOUCH,* DONALD M. HUNTEN,† GASTON KOCKARTS,‡ AND ATHENA COUSTENIS*

*Département de Recherches Spatiales, Observatoire de Paris—Meudon, F-92195 Meudon Principal Cedex, France; †Lunar and Planetary Laboratory, University of Arizona, Tucson, Arizona 85721; and ‡Institut d'Aéronomie Spatiale de Belgique, 3, avenue Circulaire, B-1180 Bruxelles, Belgium

Received January 26, 1989; revised July 5, 1989

We have reexamined the aeronomic model of Titan's thermosphere by A. J. Friedson and Y. L. Yung (*J. Geophys. Res.* 89, A1, 85–90). Our computations disagree with theirs on the evaluation of the solar heating profile. We attribute this discrepancy to a numerical error in their code. Moreover, new measurements on acetylene relaxation incite us to reconsider also their formulation of the (C_2H_2-dominated) infrared cooling. Once these factors are corrected, resolution of the heat transfer equation leads to a profile in severe conflict with the *Voyager* UVS temperature measurement at 1265 km from Titan's surface. A possible way to solve this problem is to assume very low (~0.15–0.20) heating efficiencies. Simple considerations on the UVS measurements of temperature and N_2 and CH_4 densities, together with qualitative results from the aeronomic model and constraints from the *Voyager* IRIS observations in the methane ν_4 band allow one to infer the general shape of Titan's atmosphere thermal profile. Possible features of this profile are a quasi-isothermal region between 200 and 400 km and a 135°K mesopause at 800 km.

1. INTRODUCTION

The *Voyager* mission has brought major progress to our knowledge of the Titan atmosphere. High-quality radio-occultation data allowed the inference of the thermal profile between the ground and 200 km (Lindal *et al.* 1983). Recently, a simultaneous analysis of these data and of the ν_4 emission of methane at 7.7 μm, as observed by the *Voyager* IRIS experiment, has led to a rigorous estimate of the uncertainty on the thermal profile and to the definition of a "standard" profile in this altitude range (Lellouch *et al.* 1989). The region where thermal information can be retrieved from the ν_4 emission of methane actually extends from about 150 to 400 km (Coustenis *et al.* 1989). Above 200 km, data are restricted to the solar occultation profiles obtained by the *Voyager* Ultraviolet Spectrometer (UVS) experiment (Smith *et al.* 1982). Entry and exit occultations occurred near the Equator (at 2.7°N and 17.5°S latitudes, respectively). At 1265 km, the number density was found to be $2.7 \pm 0.2 \times 10^8$ cm^{-3}, and the temperature was equal to 186 ± 30°K; these values are the average of entry and exit profiles. The major gas is N_2; CH_4 was detected at 1115 km with a 8 ± 3% mixing ratio. Smith *et al.* (1982) also report the detection of acetylene in this altitude range, with a mixing ratio of 1–2% above ~850 km altitude and 0.1–0.3% below 700 km. Isothermal interpolation down to temperature and density conditions at 200 km requires a mean temperature of 165°K between 200 and 1265 km, as pointed out by Smith *et al.* (1982).

The heat budget of the thermosphere was first investigated by Friedson and Yung (1984). Using the density and temperature values quoted above as boundary conditions, and through simultaneous solution of

0019-1035/90 $3.00

heat transfer and hydrostatic equilibrium, they predicted the shape of the thermosphere temperature profile down to the mesopause, which they estimated to occur at 736 km and 110°K. We have found, however, that this work is questionable in some aspects that we discuss below. Moreover, temperature profiles proposed subsequently for the whole 0–1300 km atmosphere (Hunten 1987, Lellouch and Hunten 1987), based on Friedson and Yung's (hereafter referenced as FY) work, contain high stratospheric temperatures to compensate for the very cold mesopause region. Coustenis and Gautier (1987) indicate that such profiles are too warm in the 200–400 km region to be consistent with the 7.7-μm emission of CH_4, as observed by *Voyager* IRIS.

Besides the interesting theoretical problem, and possible comparisons with other planets, there is at least one other reason justifying efforts to predict the temperature (and density) profile of Titan's atmosphere: in the framework of the ESA–NASA *Cassini* space mission to the Saturn system, such studies are essential for a Titan Probe mission analysis, including estimates of the Probe descent velocity and heating profile, and also for studies related to Orbiter–atmosphere interactions, such as drag during passes through the upper atmosphere and spacecraft–induced glow phenomena (Lellouch 1989).

In this work, we reexamine the aeronomic model proposed by Friedson and Yung and show that some assumptions must be modified to obtain a sensible solution. We then propose a temperature profile for the entire Titan atmosphere. Results are briefly discussed in the last section.

2. THERMOSPHERIC MODEL

The thermospheric model by FY solves the one-dimensional heat equation after evaluation of the energy sources and sinks. The main source of energy in the thermosphere is solar radiation, with a possible contribution due to precipitation of magnetospheric electrons. Solar heating is considered to occur only through gaseous absorption of solar radiation, i.e., aerosol heating is neglected. Other possible sources of heating (such as viscous dissipation of internal gravity and acoustic waves, Joule heating . . .) are omitted. Heat is radiated through infrared emission of minor constituents, and transported by molecular conduction. Eddy conduction is neglected. Following the results of Smith *et al.* (1982), three constituents are considered in the model: N_2, CH_4, and C_2H_2. The total pressure and the mixing ratios at the lower boundary of the model (680 km) are adjusted so that the calculated abundances in the heterosphere (which are of course temperature-dependent) match the observed values.

2.1. Solar Heating

Solar radiation is significantly absorbed in the thermosphere from the extreme ultraviolet (EUV) to about 2000 Å. As pointed out by FY, the most important part of heating occurs through absorption of Ly α by methane. Heating by nitrogen absorption is globally weak because it occurs below 1000 Å, where the solar flux is low. However, high above the mesopause (i.e., at altitudes $\geq$1000 km), the contribution of nitrogen to heating is dominant (Fig. 2) and therefore plays a very important role in determining the exospheric temperature. A considerable part ($\geq$20%) of the nitrogen heating is due to the absorption of solar radiation in the He II line at 303.78 Å. Acetylene absorption between 1500 and 2000 Å is negligible above 1000 km, but dominant below 800 km, where the atmosphere is opaque at all shorter wavelengths.

The most difficult factor needed to calculate the solar heating profile is the efficiency, i.e., the fraction of the photon energy actually transferred to the atmosphere after absorption. Through a detailed analysis of the dissociation channels of methane at Lyman α, FY evaluated the heating efficiencies at various wavelengths. In the ab-

sence of laboratory measurements, it is difficult, however, to estimate the quality of such an evaluation. In our model, we have assumed a linear dependence of the efficiency on wavelength. This simplified parameterization, which physically means that any photon energy greater than a given threshold is transformed into heat, is used in most of the early models of the Earth's thermosphere (Johnson and Gottlieb 1970). More realistic descriptions of the thermalization of the EUV heating must take into account the partitioning of excitation between vibrational and rotational energy, the quenching of rotational states, and the collisional deexcitation of the photodissociation products. Resulting heating efficiencies are functions of wavelength, pressure, and temperature. However, such a sophisticated approach is not only very difficult to achieve, but also probably irrelevant in the framework of this simple 1-D model, which in particular considers molecular absorption of solar radiation as the only source of energy, and neglects all dynamical phenomena. Our heating efficiency is simply

$$\varepsilon = 1 - \lambda/\lambda_0, \quad \text{for } \lambda \leq \lambda_0$$
$$\varepsilon = 0 \quad \text{otherwise,}$$

where λ is the incident photon wavelength.

For N_2, the threshold wavelength is $\lambda_0 =$ 1265 Å, corresponding to a bond energy of 226 kcal mole^{-1}, and giving $\varepsilon = 0.76$ at 304 Å. For CH_4 and C_2H_2, we use $\lambda_0 = 1870$ and 3000 Å, respectively, to be consistent with FY evaluations.

An order of magnitude of the maximal solar heating can be evaluated simply:

The contribution of Lyman α absorption by CH_4 to the solar heating at solar zenith angle θ and altitude z can be expressed as

$$S^{\alpha}_{CH_4}(z, \theta) = \varepsilon^{\alpha} F^{\alpha}_{\infty} \frac{hc}{\lambda^{\alpha}} n_{CH_4}(z) \sigma^{\alpha} \exp(-\tau^{\alpha}(z)\chi(\theta)) \quad (1)$$

where $\tau = n\sigma H$ is the opacity in vertical viewing, n is the CH_4 number density, and χ is the airmass factor or Chapman function. H is the scale height, typically equal to 80 km in the thermosphere.

This contribution is maximal at an altitude z such that $\tau = 1/\chi$ and is then equal to

$$S_{max} = \varepsilon^{\alpha} F^{\alpha}_{\infty} \frac{hc}{\lambda^{\alpha}} (e\chi H)^{-1}.$$

With a solar flux $F^{\alpha}_{\infty} = 5.5 \times 10^{+9}$ photon cm^{-2} sec^{-1} at Lyman α (solar maximum, valid for *Voyager 1* encounter), and an efficiency $\varepsilon^{\alpha} = 0.35$ (value estimated by FY), we find that for $\theta = 60°$ ($\chi = 2$), S peaks at 7×10^{-10} erg cm^{-3} sec^{-1}, which is already a factor of 5 higher than the value given by FY for the maximal value of the total solar heating (see Fig. 2 of FY). We have checked with the authors that the discrepancy comes from an error in their numerical calculation of the heating profile (J. Friedson, private communication). Unfortunately, this miscalculation has important consequences for the computation of the thermospheric profile, as shown below.

We have computed the contributions of N_2, CH_4, and C_2H_2 to the solar input profile as a function of altitude between 680 and 1400 km, with the vertical profiles displayed in Fig. 1. The CH_4 distribution adopted corresponds to a 2.5% mixing ratio in the homosphere, increasing up to ~8% at 1115 km by mass fractionation. The C_2H_2 mixing ratio is taken at 1.5% above the homopause and decreases down to 2×10^{-3} at 700 km, consistent with Smith *et al.* (1982). It must be noted that, on the basis of an evolved photochemical model, Yung *et al.* (1984) have predicted much lower C_2H_2 abundances than observed by Smith *et al.* and have questioned the C_2H_2 detection and suggested that the spectral features attributed to acetylene actually belong to other, heavier, hydrocarbons. However, according to Nava *et al.* (1986), Yung *et al.* (1984) used a rate constant for the H + C_4H_2 reaction, approximately a factor of 40 too large. With the Nava *et al.* experimental rate, much higher C_2H_2 abundances would be expected. Using solar fluxes taken from Mount and Rottman (1981) and

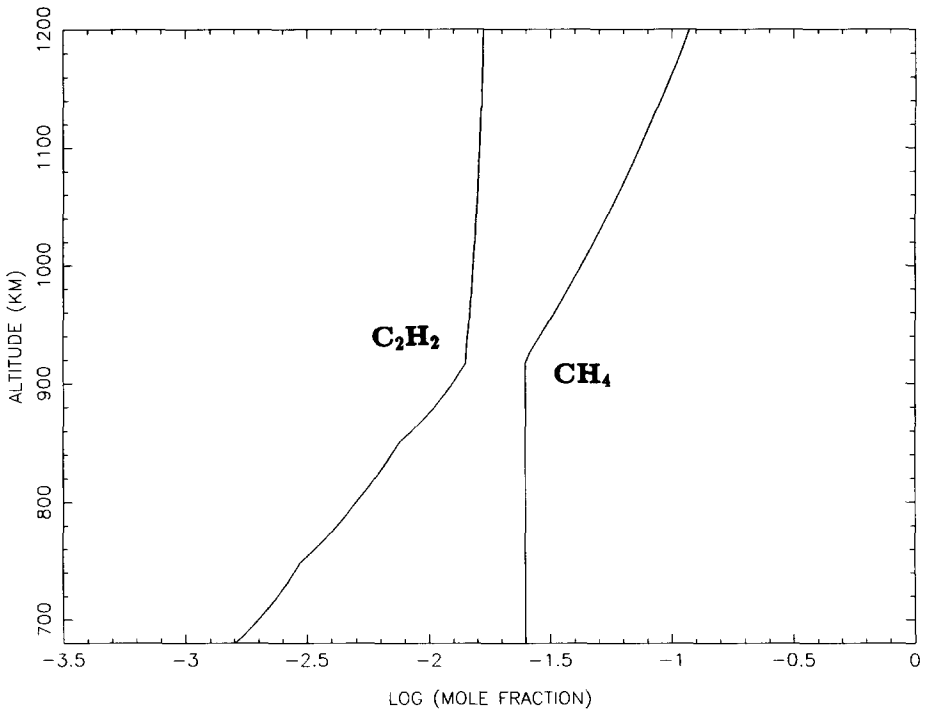

FIG. 1. Methane and acetylene distributions used in the computation of the temperature profile.

Torr and Torr (1985), we obtain the heating profiles of Fig. 2, where the total heating profile is also displayed and compared with the one computed by FY (their Fig. 2).

As said above, another possible source of heating is the low-energy magnetospheric electron precipitation. FY point out the difficulty of a quantitative evaluation of this contribution, because of the uncertainties on the electronic flux energy distribution and geometry, the heating efficiency for electron impact and the electron absorption cross sections. Their electronic heating profile is ~20% of the solar input, and thus, taking into account their error on the latter, only a few percent of the total heating. However, Hunten *et al.* (1984) have estimated that the energy deposition due to electronic precipitation is 0.015 erg cm^{-2} sec^{-1} averaged over the satellite at the exobase. When adjusted by a suitable efficiency, this energy is not negligible compared to the integrated solar heating rate (0.045 erg cm^{-2} sec^{-1} at 800 km for the profile of Fig. 2), and taking into account the fact that it is deposited at higher altitudes (1300–1500 km), it may have a significant influence on the high thermosphere profile. Our justification for omitting this contribution is that we will demonstrate (2.3) that with current values of the solar heating efficiencies, the solar energy deposition alone is already too large to be consistent with the observed exospheric temperature.

2.2. *Infrared Cooling*

Heat is removed from the upper atmosphere by nonlocal thermodynamic equilibrium (NLTE) cooling by minor constituents (Chamberlain and Hunten 1987). As pointed out by FY, the 7.7-μm fundamental of CH_4 is at too high a frequency to be strongly excited at Titanian temperatures and the 13.7-μm band of C_2H_2 dominates the cooling. FY used laboratory measurements at room temperature and the stan-

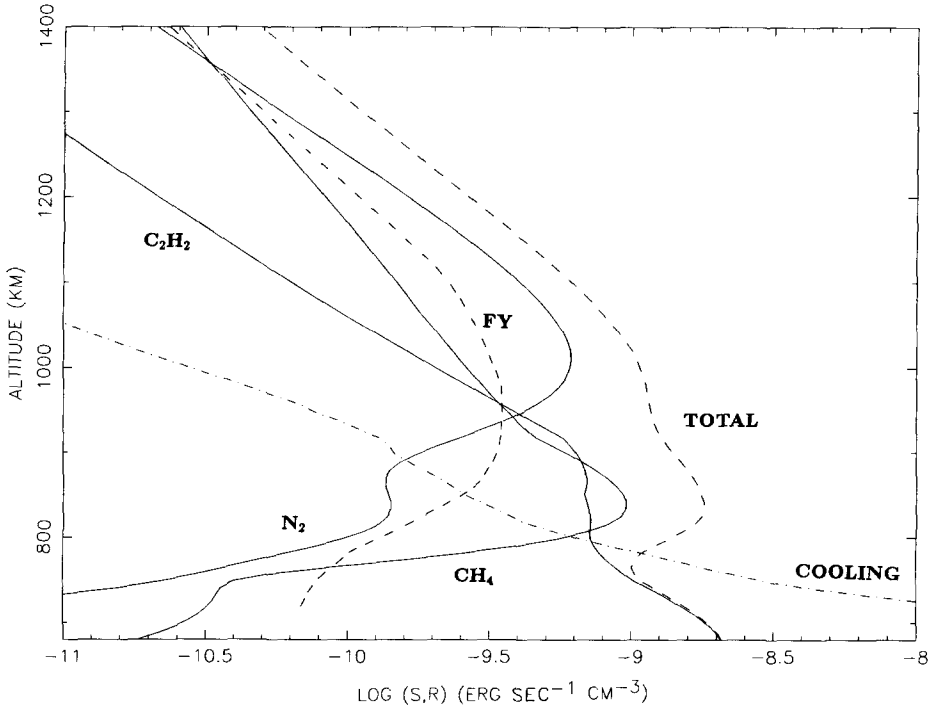

FIG. 2. Solar heating S and infrared cooling R profiles, computed with Friedson and Yung's (1984) thermospheric temperature profile (pressure: $p = 1.5 \times 10^{-7}$ bar at 680 km). The heating profile is computed for maximal solar flux and zenith angle of 60°. Solid lines: contribution of N_2, CH_4, and C_2H_2 to solar heating. Dashed lines: total solar heating, compared with Friedson and Yung's (1984). Dashed–dotted line: cooling profile.

dard (so-called Landau–Teller) temperature dependence to derive expressions of the collisional relaxation rate as a function of temperature. For both molecules, however, we have found discrepancies between their formulation and experimental data.

For methane, their formula (7) gives a value of the relaxation rate of the ν_4 band at room temperature too small by a factor of 5 if compared to the measurement by Yardley *et al.* (1970) and by a factor of 20 if we refer to Wang and Springer's (1977) results. (Note, however, that Wang and Springer's measurements were performed in CH_4-dominant (maximum N_2 proportion: 30%) CH_4–N_2 mixtures and are difficult to extrapolate to N_2–dominant mixtures; besides, the temperature dependence they quote is nonstandard.)

For acetylene, the relaxation rate of the ν_5 band at 13.7-μm, calculated at room temperature from expression (8) of FY (430 sec^{-1} $Torr^{-1}$) falls below the observed value of Häger *et al.* (1981) by a factor of 3. (A detailed study of FY calculations showed that in both cases, the discrepancy comes from an error in their computation of the kinetic collision rate Z, due to an inappropriate choice of the collision diameter of the CH_4–N_2 and C_2H_2–N_2 pairs.) Moreover, recent measurements on C_2D_2 relaxation in N_2 by Smith *et al.* (1985), giving deactivation rates higher than Häger *et al.*'s value by a factor of 5, led the authors to seriously question the work of Häger *et al.* (I. W. M. Smith, private communication). Indeed, Häger *et al.* used a 3-μm laser flash to excite the coupled levels ν_3 and $(\nu_2 + \nu_4 + \nu_5)$. The molecules rapidly decayed into the fundamentals ν_2, ν_5, and ν_4, with excitation en-

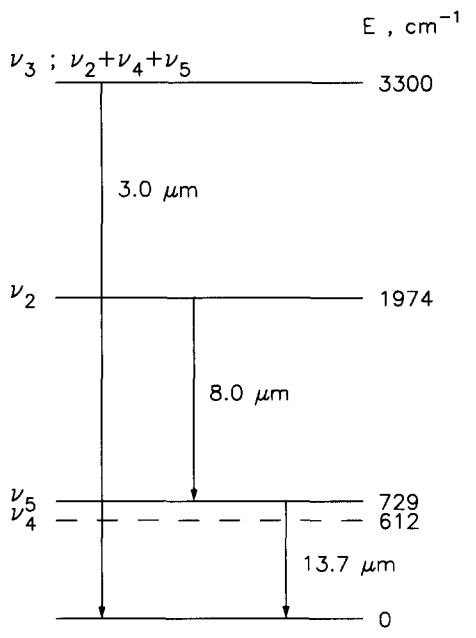

FIG. 3. Simplified energy diagram for acetylene (adapted from Häger *et al.* 1981).

ergies of 1974, 729, and 612 cm^{-1} (Fig. 3). The last is infrared inactive. The relaxation was monitored by the fluorescence of the ν_5 state as a function of pressure. Smith *et al.* (1985) point out the difficulty of quantitative fluorescence measurements. Moreover, the ν_4 and ν_5 states lie only 117 cm^{-1} apart—which corresponds to a temperature difference of 168°K—and could be collisionally coupled, at room temperature and Titanian temperatures as well. If so, the interpretation of the observed decay rate as referring to ν_5 only is not unique. For their C_2D_2 measurements, Smith *et al.* (1985) used a photoacoustic method (the relaxation is measured through microphone monitoring of the pressure change, which is directly related to the energy released into the translational degrees of freedom of the gases) which is less subject to technical problems and ambiguities of interpretation. The rate coefficient for exciting the upper level, which then radiates, can be expressed as a product of a deexcitation (quenching) coefficient and the Boltzmann factor of the upper state.

In the assumption where collisions are brief, theory (Lambert 1977) predicts a (so-called Landau–Teller) standard $T^n \exp(-A/T^{1/3})$ dependence of the relaxation rate k, where $n = 0.5$ if k is expressed in cubic centimeters per second. The A parameter depends on the frequency of the band, on the reduced mass of the colliding partners, and on a typical length characterizing the interaction potential range, and cannot be calculated ab initio. At high temperature, the standard temperature dependence is observed in most of the cases. To our knowledge, no experimental data are available on the relaxation of methane and acetylene at low temperatures. Yuan *et al.* (1973) have performed measurements on the relaxation of ethylene in rare gases, at various temperatures, down to 248°K. For C_2H_4 relaxation in Ne, they obtain $A = 35$. We shall first assume that the same dependence is valid for relaxation of CH_4 and C_2H_2 in N_2. We thus use, as a starting point, the following expressions for the relaxation coefficients:

$$k(CH_4\text{–}N_2) = 2.25 \times 10^{-14} T^{0.5} \exp(-35/T^{1/3}) \quad cm^3\ sec^{-1}$$

$$k(C_2H_2\text{–}N_2) = 1.9 \times 10^{-12} T^{0.5} \exp(-35/T^{1/3}) \quad cm^3\ sec^{-1}.$$

At 170°K, these expressions, compared to the ones in FY, give relaxation coefficients higher by a factor of 10 for both molecules. At this point, we stress that our adopted expressions are highly uncertain. Accordingly to one of the referees (D. F. Strobel), it is very improbable that the Landau–Teller dependence is valid for colliding linear molecules at low temperatures, as indicated by the behavior of CO_2, whose deactivation probabilities with various partners below 240°K are much less temperature-dependent than predicted by the standard dependence (Allen *et al.* 1980). In the absence of any firm information on C_2H_2, we will later test different values of the relaxation rate with N_2. The cooling rate per

molecule in a band at frequency ν can be expressed as a function of the relaxation coefficient k and of the radiative transition probability A, (Kockarts 1980)

$$R = h\nu\omega A \frac{g_1}{g_0} \exp\left(-\frac{h\nu}{kT}\right), \quad (2)$$

where g_1 and g_0 are the degeneracies of the upper and lower levels of the transition, and $\omega = k(T)N/(k(T)N + A)$ is a dilution factor from the LTE case (N is the total ambient density). This expression assumes that radiation in both the upward and downward directions cools the atmosphere, and holds in the isotropic "cool-to-space" approximation, which is valid if $\bar{\tau}A/kN \gg 1$, where $\bar{\tau}$ is the probability of photon escape to space (Houghton 1986). Using a band model formulation, we find that for the ν_5 band of acetylene, this inequality occurs at $z \geq 750$ km. Below this level, the cool-to-space formulation provides an upper limit of the cooling rate. To account for the collisional coupling of the ν_4 and ν_5 bands, we use a degeneracy g_1 equal to 4 (2 for each level). The cooling rate profile computed with these coefficients, the molecular profiles of Fig. 1, and the thermal profile of FY is displayed in Fig. 2.

2.3. *Computation of the Thermospheric Profile*

With the heating efficiencies and relaxation coefficients given above, and the vertical distributions of methane and acetylene as shown in Fig. 1, we now compute the temperature profile of the thermosphere, with the same type of boundary conditions as in FY. We actually compute the diurnally averaged thermal profile, through the simplified conduction equation, in spherical coordinates,

$$-\frac{d}{dr}\left(K(T)r^2\frac{dT}{dr}\right) = r^2(S - R), \quad (3)$$

where $K(T)$ is the thermal conductivity of the atmosphere, S is the diurnally zenith angle averaged solar heating profile, R is the diurnally averaged radiative losses, and where the contribution to heating due to electron precipitation has been neglected. $K(T)$ is calculated as the weighted average of the conductivities of the three gases. For the conductivity of N_2, we used Eq. (8) of FY, which is an excellent simple approximation of experimental data in the relevant temperature range (50–300°K). The conductivities of CH_4 and C_2H_2 were assumed to follow the same temperature dependence and were taken as 1.12 and 0.65 times the conductivity of N_2, respectively (Weast 1981).

Strictly speaking, the exact computation of the diurnal averages of the heating and cooling terms in Eq. (3) would require knowledge of the temperature profile as a function of local time, but this in turn would imply solution of the time-dependent heat equation. Instead, diurnal averages have been calculated from Eqs. (1) and (2), with T being the diurnally averaged temperature. For the solar input average, the solar-time dependent $\exp(-\tau(z)\chi(\theta))$ term was calculated for 24 values of the airmass factor (one per hour, $\chi(\theta)$ being infinite when the considered altitude is in the night). For the cooling rate, the strong non-linear dependence of k and R with T makes the method approximate. An estimate of the error can be obtained by comparing the cooling rate at 180°K with its averaged value between 150 and 210°K, which may be the range of diurnal variation of the exospheric temperature, as found by FY. We find a difference of about 20%, which is negligible in view of the much larger uncertainty (factor 2–5?) on the relaxation coefficients. Since K, S, and R are all functions of T, Eq. (3) is solved iteratively. The problem is entirely defined with two boundary conditions: at the upper level of the model, the second member of the equation vanishes, and it may be assumed that $dT/dr = 0$. We take the upper boundary layer at 1500 km, checking that both solar input and radiative losses are negligible at this altitude. The second boundary condition is defined by the temperature at a given level.

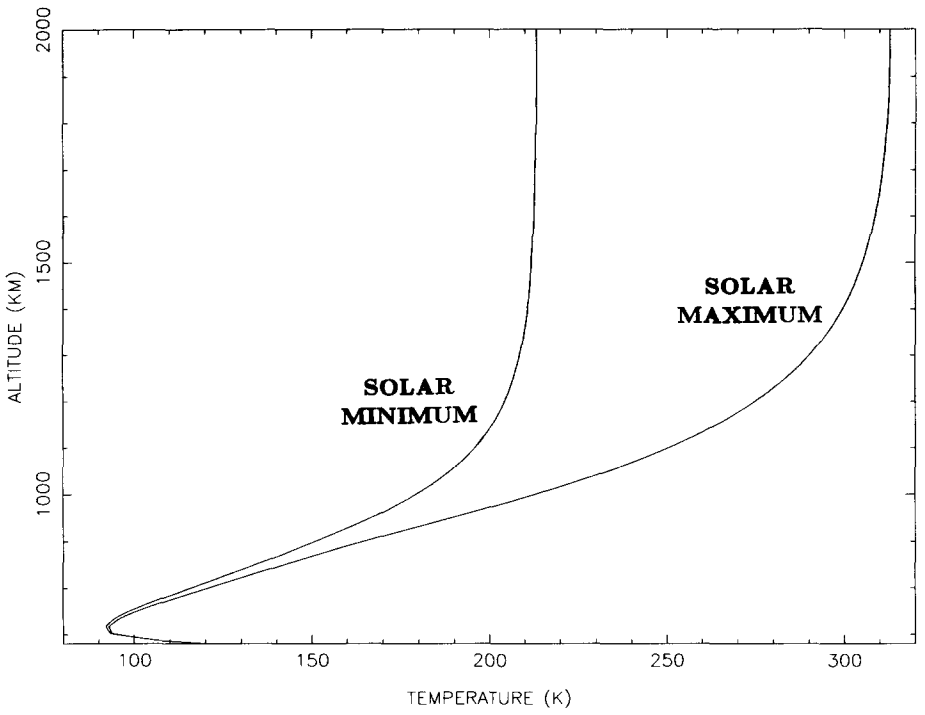

FIG. 4. Diurnal average temperature computed from Eq. (1) for maximum and minimum solar conditions.

In a first step, we use the same condition as in FY; i.e., the temperature is given at the lower boundary of the model, which is taken at 680 km (where, as shown by FY, the temperature profile has negligible diurnal variations). Since we solve simultaneously the hydrostatic equilibrium equation, the total pressure has to be given at the same level. The mole fractions of the various species must also be specified and are constrained by the UVS measurements. With the boundary conditions, $T(680\text{ km}) = 120°\text{K}$, $p(680\text{ km}) = 1.5 \times 10^{-7}$ bar, we obtain the thermospheric profiles at the Equator shown in Fig. 4, for maximal and minimal solar conditions, respectively. The *Voyager 1* encounter with Titan occurred during solar conditions very close to maximal. The computed profile is grossly inadequate. The reason for a very large temperature gradient above the mesopause, leading to extremely high (~310°K) exospheric temperatures, is the strong heating profile above 800 km. Actually, the cooling term, scaling roughly as the square of the total pressure, becomes entirely negligible above 950 km. Taking into account the electronic heating would of course lead to even higher exospheric temperatures. We have not investigated the diurnal variation of the temperature, but given the higher heating profile compared to FY, it can be expected that computation of the time-dependent heat equation would lead to a dramatic diurnal thermal variation, severely violating the UVS results.

We have studied the sensitivity of the results to the lower boundary (pressure, temperature) conditions. An increase of pressure at the lower boundary causes a larger increase in the cooling term than in the heating, and thus produces a colder mesopause. But the moderate increase of the heating term above the mesopause (due to the increase of concentrations) is such that the exospheric temperature does not

depend strongly on the pressure assumed at the lower boundary. Specifically, T_{exo} is found to vary by ±5% when p(680 km) undergoes a change by a factor of 4. (The N_2 and CH_4 concentrations measured in the thermosphere constrain p(680 km) to a precision better than this.) The temperature at the lower boundary is entirely unconstrained. FY assumed T(680 km) = 130°K. A higher value of this temperature causes a strong increase of the cooling term which compensates for this temperature, so that the temperature at the mesopause (and thus everywhere above) appears to be almost independent of the temperature lower boundary condition, as found by FY. On the other hand, the CH_4 and C_2H_2 mole fractions assumed below the mesopause do have a strong influence on the thermospheric profile, but they are also relatively well constrained (especially CH_4) by the UVS measurements.

Therefore, we find that, to obtain a sensible thermospheric profile, we have to modify either the heating term (through the heating efficiencies) or the cooling term (through the relaxation rates) or both of them. Since the profile we first obtained was much too hot, we must try to reduce the solar input or increase the radiative losses. Thus, in a second step, instead of FY's method, used above, we now integrate the equation of conduction (1) (again, neglecting electronic heating) downward from 1265 km, with the UVS measurements (T = 186°K, $[N_2] = 2.7\ 10^8$ cm^{-3}) and again $dT/dr = 0$ at this point as boundary conditions.

We first assume that the expression for the cooling term is valid, and we compute the thermospheric profile, starting from 1265 km, for heating efficiencies reduced arbitrarily by various factors. Figure 5 shows the results. The smaller the efficien-

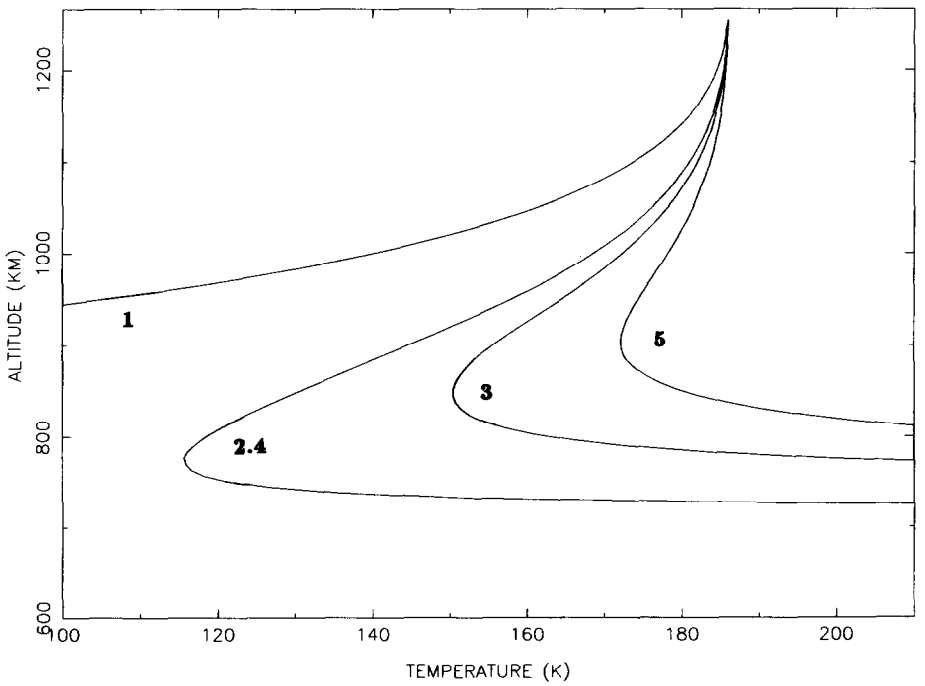

FIG. 5. Thermospheric profile computed downward from the UVS point (T = 186°K, $[N_2] = 2.7 \times 10^8$ cm^{-3} at 1265 km) for various reduction factors of the solar heating efficiencies from their nominal values. Labels indicate the reduction factors. Cooling rates are nominal.

cies, the smaller the integrated solar flux and thus the temperature gradients, and since we integrate downward, with a fixed point at 1265 km, the higher the thermospheric temperatures are, even though this may seem paradoxical at first glance. For efficiencies reduced by a factor of about 2.4 (i.e., for an efficiency of about 0.15 for CH_4 in Lyman α, and 0.32 for N_2 at 304 Å), a profile similar to FY's is obtained. That cannot be related directly to the difference in the solar heating profile (factor of about 7, as shown in Fig. 2), because the discrepancy on the relaxation rates (factor 10) also plays a role. The same thermosphere profile can be obtained assuming a global heating efficiency of 0.19, independent of molecule or wavelength. This value is significantly smaller than the ones proposed by FY for CH_4 absorption (0.35 in Ly α and 0.40 at other wavelengths), and it seems very difficult to find a theoretical model predicting such a low CH_4 efficiency (A. J. Friedson, private communication). However, it appears that absorption by CH_4, although globally dominant, is not the most important in determining the thermospheric profile. The reason for this is that it occurs at relatively low altitudes (800–900 km), where a large fraction of the heat can be removed from the atmosphere by infrared cooling. Instead, the exospheric temperature is primarily a function of the N_2 heating at EUV wavelengths (150–350 Å), and provided the assumed relaxation rates are correct, efficiencies in the 0.2–0.4 rather than in the 0.7–1 range are needed.

We next compute the thermospheric profiles with the efficiencies used in the beginning, exploring a range of values of the relaxation rate of acetylene, since methane contribution to the cooling is small. For simplicity, we assume a constant value of the C_2H_2 relaxation rate at all temperatures. In other words, we are testing various values of the relaxation rate of acetylene by nitrogen around 170°K. Results are shown in Fig. 6, and compared with the "nominal" C_2H_2 relaxation rate (which includes the temperature dependence). Rate coefficients of at least 5×10^{-13} cm^3 sec^{-1} are needed to produce a sensible solution, i.e., a factor of at least 10 higher than the value used initially (5×10^{-14} cm^3 sec^{-1} at 170°K).

Finally, we have tested several values of the C_2H_2 relaxation rate, assuming reduction of the heating effiencies by a factor of 2.4. As shown in Fig. 7, various possible solutions are obtained for a rate coefficient ranging from 2×10^{-14} to 10^{-12} cm^3 sec^{-1} at 170°K.

It must be noted that, due to the rapid increase of the cooling term downward (due to the increase of pressure, and even though the C_2H_2 mixing ratio probably decreases), all computed profiles show an extremely strong negative gradient just below the mesopause. Since the gradient cannot exceed the adiabatic lapse rate, which is 0.87°K/km at 600 km, this indicates the limitations of the model. In particular, infrared opacities become nonnegligible below the mesopause and departure from the "cooling-to-space" regime should be considered, acting as an effective heating source. Moreover, there may be substantial heating by near-infrared bands of methane and by dust particles, both of which can absorb solar energy.

To conclude at this point, the model shows that the thermosphere structure of Titan is extremely sensitive to the solar heating efficiencies and to the relaxation rates of the cooling agents. Given our poor knowledge of these parameters, almost any thermal profile can be obtained theoretically, and the only firm achievement of the model seems to demonstrate the existence of a mesopause, which is due to the very efficient cooling in the C_2H_2 ν_5 band.

3. POSSIBLE PROFILE OF TITAN'S ATMOSPHERE

In this section, we put together the results of the thermospheric model given above and other independent observational constraints in order to propose a profile of Titan's atmosphere, from the ground to the

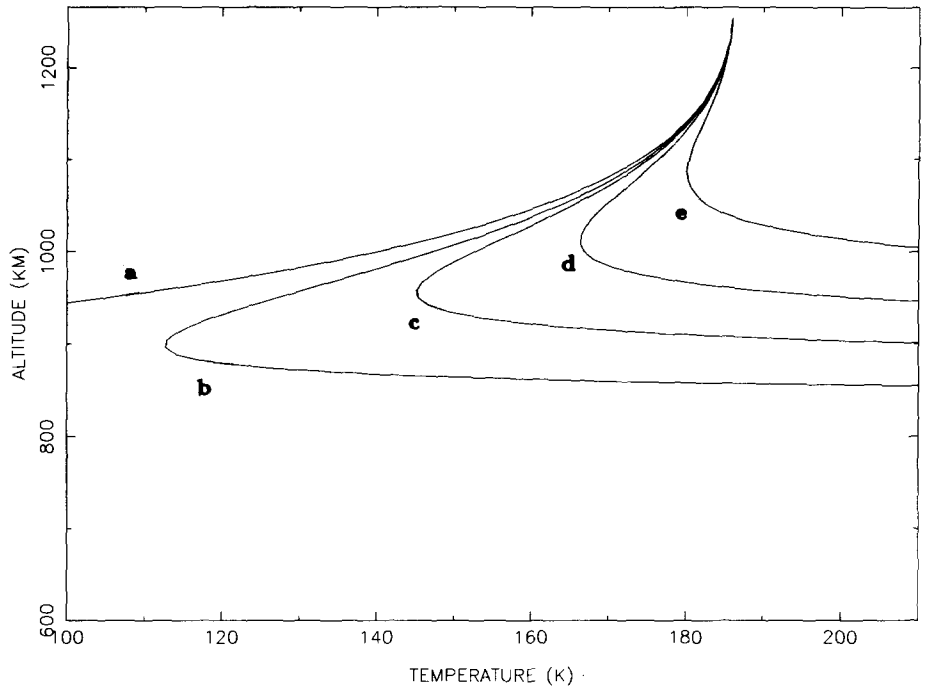

FIG. 6. Same as Fig. 5, but for nominal heating efficiencies and various C_2H_2 relaxation rates k. (a) $k = 1.9 \times 10^{-12}\, T^{0.5} \exp(-35/T^{1/3})$ cm^3 sec^{-1} (nominal), (b) $k = 6 \times 10^{-13}$ cm^3 sec^{-1}, (c) $k = 1 \times 10^{-12}$ cm^3 sec^{-1}, (d) $k = 2 \times 10^{-12}$ cm^3 sec^{-1}, (e) $k = 5 \times 10^{-12}$ cm^3 sec^{-1}.

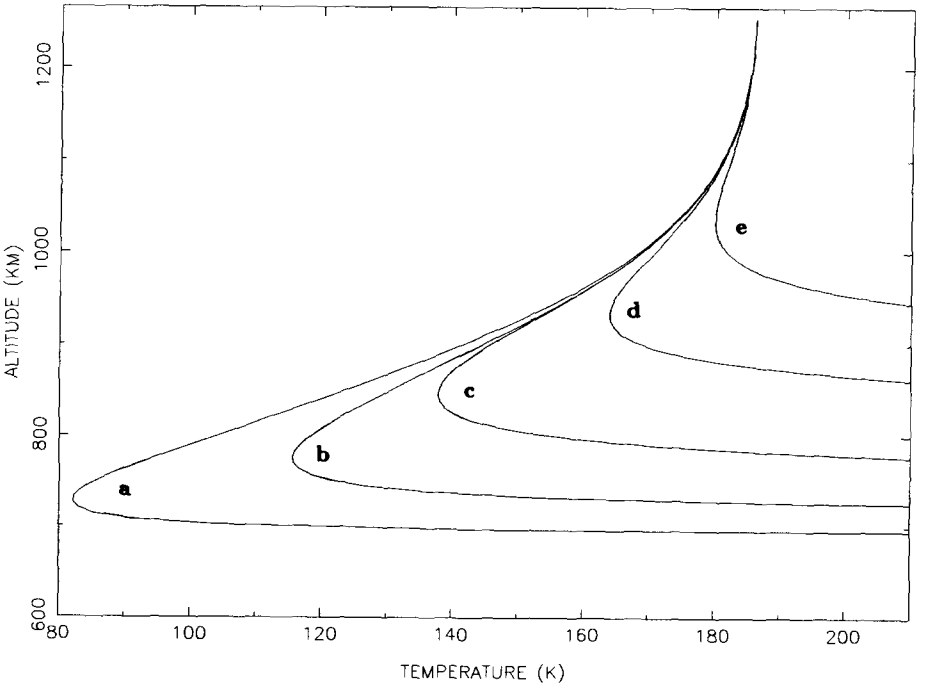

FIG. 7. Same as Fig. 6, but for heating efficiencies reduced from their nominal values by a factor 2.4 (a) $k = 2 \times 10^{-14}$ cm^3 sec^{-1}, (b) $k = 1.9 \times 10^{-12}\, T^{0.5} \exp(-35/T^{1/3})$ cm^3 sec^{-1} (nominal), (c) $k = 5 \times 10^{-14}$ cm^3 sec^{-1}, (d) $k = 2 \times 10^{-13}$ cm^3 sec^{-1}, (e) $k = 10^{-12}$ cm^3 sec^{-1}.

exosphere. The *Voyager* UVS experiment (Smith *et al.* 1982) measured the temperature and the nitrogen number density at 1265 km, and the methane concentration (1.2×10^8 cm^{-3}) and mixing ratio ($8 \pm 3\%$) at 1115 km above Titans surface. Smith *et al.* inferred the homopause level to be at 925 ± 70 km.

Recently, from a joint reanalysis of the *Voyager* radio-occultation and IRIS 7.7-μm data, Lellouch *et al.* (1989) found the temperature at 200 km to be 173 ± 4°K. The methane mole fraction in the uniformly mixed stratosphere is bounded between 0.5 and 3.4%, and between 1 and 1.7% if no significant argon is present in the atmosphere.

Let us assume that the CH_4 mixing ratio in the low stratosphere, q_1, is constant up to the homopause (altitude z_h), and then increases to a value q_2 at 1115 km. This simplified model is supported by the results of the photochemical model of Yung *et al.* (1984). In this framework, the densities and temperature measured by UVS allow evaluation of the most reasonable values of q_1, q_2, and z_h. Indeed, each set (q_1, q_2, z_h) provides a value of the average temperature between z_h and 1115 km: T_2. Furthermore, q_2 and the methane concentration at 1115 km provide the N_2 concentration at 1115 km, which in turn gives the average temperature between 1115 and 1265 km: T_3 (see Fig. 9).

Coustenis *et al.* (1989) show that the ν_4 emission of CH_4 at 7.7-μm observed by IRIS is compatible with a CH_4 mole fraction of 1.8%, and a profile with temperatures of 170°K at 200 km, 176°K at 250 km, and 180°K at 350 km and above. From the error bars on the temperature at 200°K found by Lellouch *et al.* (1989), we conclude that the average temperature between 200 and 500 km is most probably higher than 175°K. This shows that the CH_4 mixing ratio in this altitude range cannot be much higher than 1.8%. We therefore explored the three-dimensional domain where q_1 varies from 0.5 to 2.5%, q_2 from 5 to 11%, and z_h from 855 to 995 km, calculating T_2 and T_3 for each set (q_1, q_2, z_h). No argon was assumed. Reasonable constraints on T_2 and T_3 ($T_2 \geq 120$°K; $T_2 \leq T_3$; 155°K $\leq T_3 \leq 215$°K), based on observational results and qualitative properties of the thermospheric profile, as found in Section 2, were used to find a plausible range for the three parameters. For example, low values of q_1 and high values of z_h are excluded because they lead to unacceptably low values of T_2; $T_3 \leq 215$°K imposes $q_2 \leq 10\%$. Figure 8 shows, for various values of z_h, the most "reasonable" couples (q_1, q_2). The most satisfactory solutions are obtained for large values of q_1, but such values tend to be excluded by the analysis of Coustenis *et al.* (1989). Moreover, in the absence of argon, stratospheric CH_4 mole fractions higher than 1.7% would imply supersaturation of CH_4 with respect to the condensation level (32 km) value. We finally adopt $q_1 = 1.7\%$, $q_2 = 7\%$, and $z_h = 880$ km as the "best" solution. The corresponding average temperatures are $T_1 = T(200\text{–}880 \text{ km}) = 160$°K, $T_2 = T(880\text{–}1115 \text{ km}) = 169$°K, and $T_3 = T(1115\text{–}1265 \text{ km}) = 180$°K.

Simple consideration of these numbers shows that there must be a mesopause somewhere in the atmosphere, in agreement with the prediction of the aeronomic models, and that it is most probably located below the homopause level, since $T_1 \leq T_2$. The fact that T_3 is not close to T_2 implies a significant temperature gradient in the 1100–1200 km range and would indicate that the profile becomes isothermal only well above 1265 km.

A smooth profile was then obtained by trial and error, which satisfies the hydrostatic equation (Fig. 9). It shows a cold mesopause at about 800 km and 135°K. To compensate for the low temperatures around the mesopause, the warm region in the stratosphere extends up to about 500 km. Below 200 km, the temperatures follow the standard profile of Lellouch *et al.* (1989). The 150–400 km region can be tested against 7.7-μm emission of CH_4, as

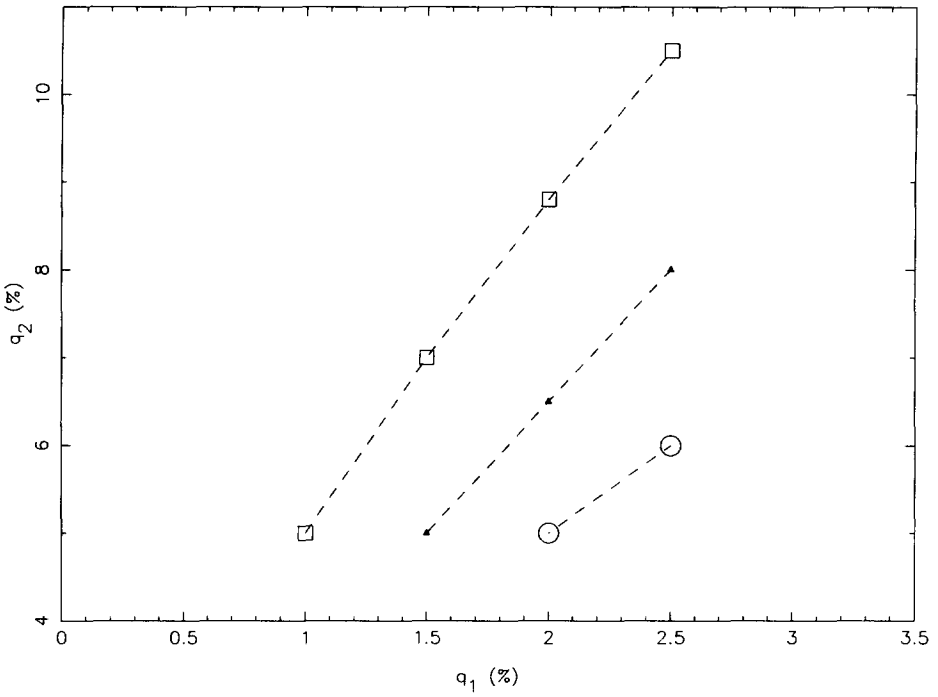

FIG. 8. For various homopause locations (z_h = 925 ± 70 km), most reasonable (q_1, q_2) couples. q_1 is the methane mixing ratio in the uniformly mixed atmosphere, q_2 is the methane mixing ratio at 1115 km. Squares: z_h = 855 km. Triangles: z_h = 925 km. Circles: z_h = 995 km.

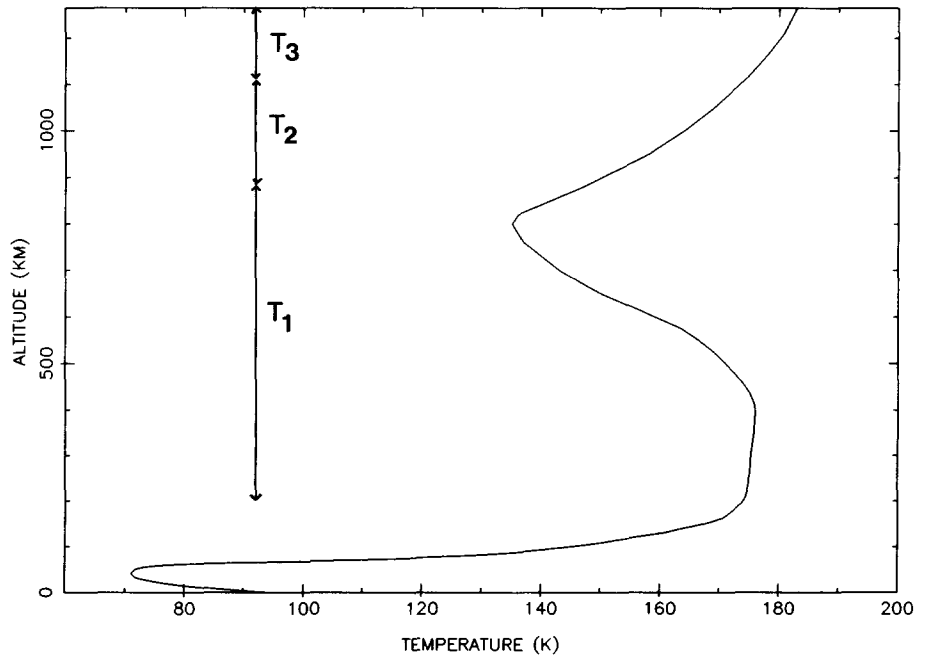

FIG. 9. Titan's proposed temperature profile. The thermospheric part of the profile is compatible with a global heating efficiency of 0.17. Arrows indicate the altitude domains whose average temperatures T_1, T_2, and T_3 have been estimated (see text).

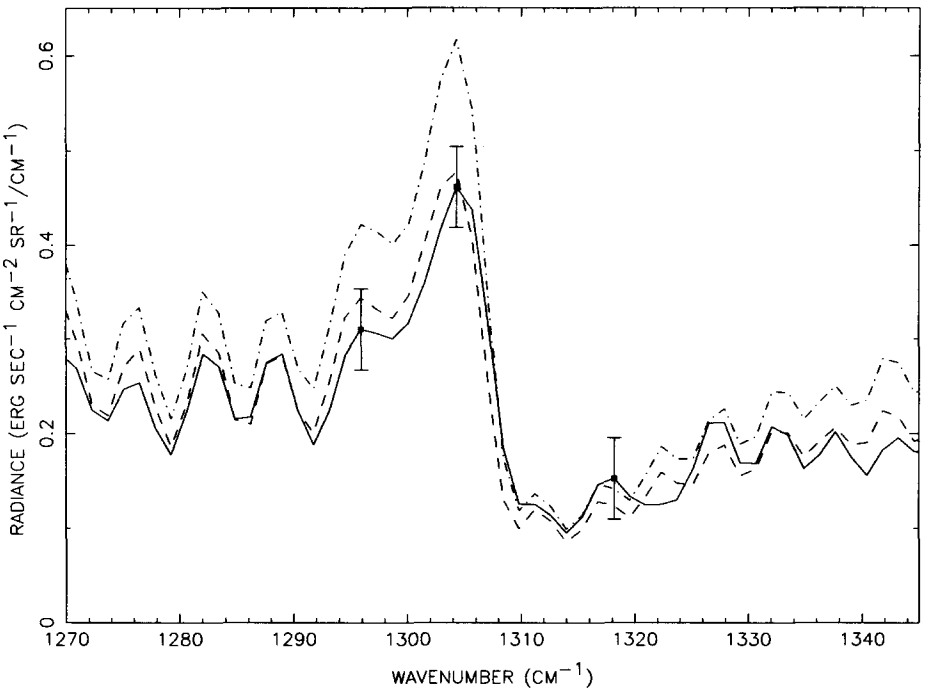

FIG. 10. Fit of the ν_4 band of CH_4 with two different thermal profiles and a CH_4 mole fraction of 0.017. Solid line: IRIS data ($\pm 3\ \sigma$ error bars are indicated). Dashed line: model, for the atmospheric profile proposed here. Dashed–dotted line: model, for a profile based on Friedson and Yung's (1984) (Lellouch and Hunten 1987).

observed by IRIS. For this purpose, a synthetic spectrum is generated, with the temperature profile and its associated methane mole fraction (1.7%), through a line-by-line radiative transfer program which computes the monochromatic radiance emerging from the atmosphere. This spectrum is compared to an average of a selection of 30 IRIS spectra taken in Titan's Equatorial region. The noise level on the resulting spectrum is about 0.014 erg cm^{-2} sec^{-1} sr^{-1}/cm^{-1}. Details of the analysis can be found in Coustenis *et al.* (1989). As shown in Fig. 10, the agreement between the observed and synthetic spectrum is satisfactory within $\pm 3\ \sigma$ error bars. Profiles with much colder mesopauses (such as FY) tend to be excluded, because they require, in order to satisfy hydrostatic equilibrium, temperatures too warm at lower levels to allow for a good fit of the ν_4 emission of CH_4 (Fig. 10).

4. DISCUSSION

Comparing the temperature profile obtained from simple arguments in the previous section with predictions of the thermospheric model should in principle give information on the physics of the thermosphere. Although the shape of the proposed profile is very uncertain and most probably criticizable, due to the absence of any constraint between 400 km and the mesopause, the temperatures above the mesopause are to some extent constrained by the UVS data, as shown in Section 3. However, the thermospheric profile (and especially the altitude and the temperature of the mesopause), as predicted from the model, is basically a function of two parameters, the heating efficiencies and the relaxation rate of C_2H_2, and it is difficult to derive information on both of them independently. Still, some qualitative results can be given:

The profile proposed in Fig. 9 has its mesopause at 800 km. A glance at the models in Figs. 5–7 shows that such a result is most readily obtained with a reduced heating efficiency. A reduction of the "nominal" efficiencies by a typical factor of 2.5–3 would be adequate, as would be a global average heating efficiency in the range 0.15–0.20. Increased cooling coefficients (Fig. 6) tend to raise the mesopause into the 900 km region or even higher. Although considerations in Section 3 tend to indicate that the mesopause is located below the homopause (~880 km), the oversimplified approach adopted there does not allow ruling out the possibility of generating a full profile corresponding to this situation. The mesopause would then be warmer and lapse rates in the mesosphere smaller. Also possible is a slightly reduced heating efficiency combined with increased cooling. For example, the cooling rate at low temperature might be essentially equal to the room-temperature value of Smith *et al.* (1985). Such cases, though not the most common, do exist: in SO_2, CH_3F, CH_3Br, the rate actually rises at lower temperatures. They are attributed to formation of a long-lived complex (Lambert 1977), a process that could also be important in the nitrogen–acetylene system.

A heating efficiency in nitrogen reduced to 0.15–0.20 seems to be in conflict with the well-established value for the Earth, where the gas is actually a mixture of nitrogen and atomic oxygen. However, the CO_2 atmospheres of Venus and Mars offer precedents. The need for low efficiencies was first realized by Stewart (1972) at Mars and Dickinson (1976) and Dickinson and Ridley (1977) at Venus, and this suggestion has been confirmed by later work. Bougher *et al.* (1988a) require 10–12% for Venus, and Bougher *et al.* (1988b) find 18% for Mars. Thus, a reduced value for Titan may not be ruled out. The best prospect for the near future is for further laboratory measurements to establish the actual cooling rate of acetylene at low temperatures.

As we said earlier, the aeronomic model described in Section 2 becomes nonvalid below the mesopause, because the computed lapse rates are superadiabatic there. This is partly due to the breakdown of the assumption that infrared optical thicknesses effects are negligible, but this probably also demonstrates the existence of a source of heating in the high mesosphere, at altitudes (600–800 km) where solar UV radiation cannot penetrate. In the absence of solar heating, the temperature of the entire stratosphere and mesosphere should approach the Gold–Humphreys skin temperature (Chamberlain and Hunten 1987), which is about 72°K if the effective temperature of Titan is 86°K. Since the actual temperature over the whole region is around 160°K, it is clear that the heating is dominated by the solar input. Short wavelength overtones of CH_4 are certainly significant, but the heating is probably dominated by absorption by the smog particles (or Danielson dust) that make Titan's albedo so low. The *Voyager* UVS experiment saw absorption layers at the limb up to 765 km, and it is likely that diffuse dust extends to 800 km or somewhat higher (Smith *et al.* 1982). There can thus be no doubt that there is major dust heating. Its amount could be in principle estimated from the proposed thermal profile, but almost any result could be obtained depending on what is assumed about the infrared cooling rates.

A final comment on the "engineering" aspect of the problem. In the baseline *Cassini* mission, the Probe will enter Titan's atmosphere with an ~7 km/sec velocity. A decelerator will reduce its speed to Mach 1.5 (~400 m/sec) at about 190 km altitude above Titan's surface. At this point, marking the end of the entry phase, the decelerator is jettisoned and the parachute deployed, and the descent phase starts. Atmospheric friction will begin at about 500 km. The Probe will undergo decelerations up to $\sim 15g$, peaking near 290 km (Flury *et al.* 1987). At the same level, the heating flux on the Probe will peak at about 46 W/cm^2

(M. Eiden, private communication). All these numbers are of course functions of the density profile between 200 and 500 km. The mission design also foresees 30 to 40 Titan flybys of the Orbiter at ~1000 km altitude. At this level, the density is about 10^{10} mol. cm^{-3}, which compares with the density in the Earth's atmosphere at 200 km. Spacecraft-induced glow phenomena have been observed in the atmosphere up to 300 km (Dalgarno 1985), which raises concern about possible similar contamination in the *Cassini* case (Lellouch 1989). Glow intensities may vary very quickly with ambient density, perhaps as its cube (Conway *et al.* 1987). This ensemble of facts illustrates the importance of a good knowledge of the Titan's atmosphere density—and therefore temperature—profile above 200 km. Further efforts to reconcile thermospheric models with *Voyager 1* data and to model the stratosphere and mesosphere profiles, together with possible new observational data, notably from stellar occultation or measurements of strong CO submillimeter lines, leading to a more reliable profile of the entire Titan's atmosphere will be most useful in the preparation of the mission.

ACKNOWLEDGMENTS

We are indebted to Jim Friedson for the time he spent discussing with us problems related to the estimation of the solar heating profile and of the relaxation rate, and for a number of interesting comments on the manuscript. We also thank Ian Smith for pointing out to us the existence of new data on C_2D_2 relaxation, Roger Yelle and Daniel Gautier for their remarks on preliminary versions of this work, and Darrell Strobel for constructive reviewing of the paper.

Note added in proof. The recent occultation of 28 Sgr by Titan on July 3, 1989 provided a unique opportunity to probe Titan's atmosphere in the 250–500 km range. Isothermal fits of occultation curves recorded at various stations in the Mediterranean area give scale heights of 53.6 ± 6 km (Sicardy *et al.* 1989, *Nature*) and 55.6 ± 3 km (Hubbard *et al.* 1989, *Nature*) at 450 km altitude. For a molecular mass of 27.84, corresponding to 1.7% CH_4 and 98.3% N_2, the corresponding temperatures are 175 ± 21 K and 182 ± 10 K, in good agreement with the model presented here (174 K at 450 km).

REFERENCES

ALLEN, D. C., T. SCRAGG, AND C. J. S. M. SIMPSON 1980. Low temperature fluorescence studies of the deactivation of the bend–stretch manifold of CO_2. *Chem. Phys.* **51,** 279–298.

BOUGHER, S. W., R. E. DICKINSON, E. C. RIDLEY, AND R. G. ROBLE 1988a. Venus mesosphere and thermosphere. III. Three dimensional general circulation with coupled dynamics and composition. *Icarus* **73,** 545–573.

BOUGHER, S. W., R. E. DICKINSON, R. G. ROBLE, AND E. C. RIDLEY 1988b. Mars thermospheric general circulation model: Calculations for the arrival of Phobos at Mars. *Geophys. Res. Lett.* **15,** 1511–1514.

CHAMBERLAIN, J. W., AND D. M. HUNTEN 1987. *Theory of Planetary Atmospheres: An Introduction to Their Physics and Chemistry,* 2nd ed., pp. 10–12. Academic Press, Orlando.

CONWAY, R. R., R. R. MEIER, D. F. STROBEL, AND R. E. HUFFMAN 1987. The far-ultraviolet vehicle glow of the S3-4 satellite. *Geophys. Res. Lett.* **14,** 628–631.

COUSTENIS, A., B. BEZARD, AND D. GAUTIER 1989. Titan's atmosphere from *Voyager* infrared observations. I. The gas composition of Titan's equatorial region. *Icarus* **80,** 54–76.

COUSTENIS, A., AND D. GAUTIER 1987. *Constraints on Titan's Atmosphere Temperature Profile from IRIS Spectra. Cassini* Science Working Group Meeting, Graz, Austria, July 9–11, 1987.

DALGARNO, A. 1985. *Second Workshop on Spacecraft Glow,* NASA-CP 2391. Huntsville, Alabama, May 6–7, 1985.

DICKINSON, R. E. 1976. Venus mesosphere and thermosphere temperature structure. I. Global mean radiative and conductive equilibrium. *Icarus* **27,** 479–493.

DICKINSON, R. E., AND E. C. RIDLEY 1977. Venus mesosphere and thermosphere temperature structure. II. Day–night variations. *Icarus* **30,** 163–178.

FLURY, W., T. PRIETO-LLANOS, AND J. DE LEEUW 1987. *Probe Mission Analysis. Cassini* Science Working Group Meeting, Graz, Austria, July 9–11, 1987.

FRIEDSON, A. J., AND Y. L. YUNG 1984. The thermosphere of Titan. *J. Geophys. Res.* **89,** A1, 85–90.

HÄGER, J., W. KRIEGER, AND J. PFAB 1981. Collisional deactivation of laser-excited acetylene by H_2, HBr, N_2 and CO. *J. Chem. Soc. Faraday Trans. 2* **77,** 469–476.

HOUGHTON, J. T. 1986. *The Physics of Atmospheres,* Pp. 61, 65. Cambridge Univ. Press, London/New York.

HUNTEN, D. M. 1987. *Titan Model Atmosphere. Cassini* Science Working Group Meeting, Graz, Austria, July 9–11, 1987.

HUNTEN, D. M., M. G. TOMASKO, F. M. FLASAR, R. E. SAMUELSON, D. F. STROBEL, AND D. J. STE-

VENSON 1984. Titan. In *Saturn* (T. Gehrels and M. S. Matthews, Eds.), pp. 671–759. Univ. of Arizona Press, Tucson.

JOHNSON, F. S., AND B. GOTTLIEB 1970. Eddy mixing and circulation at ionospheric levels. *Planet. Space Sci.* **18,** 1707–1718.

KOCKARTS, G. 1980. Nitric oxide cooling in the terrestrial atmosphere. *Geophys. Res. Lett.* **7,** 137–140.

LAMBERT, J. D. 1977. *Vibrational and Rotational Relaxation in Gases.* Clarendon Press, Oxford.

LELLOUCH E. 1989. *On the possible occurrence of spacecraft glow during the Cassini Orbiter Titan flybys.* ESTEC report, Space Science Department of ESA, ESTEC, January 1989.

LELLOUCH, E., A. COUSTENIS, D. GAUTIER, F. RAULIN, N. DUBOULOZ, AND C. FRÈRE 1989. Titan's atmosphere and hypothesized ocean: A reanalysis of the *Voyager 1* radiooccultation and IRIS 7.7-μm data. *Icarus* **79,** 328–349.

LELLOUCH, E., AND D. M. HUNTEN 1987. *Titan Atmosphere Engineering Model. E.S.A. Space Science Department Internal Publication,* ESLAB 87–199.

LINDAL, G. F., G. E. WOOD, H. B. HOLZ, D. N. SWEETNAM, V. R. ESHLEMAN, AND G. L. TYLER 1983. The atmosphere of Titan: An analysis of the *Voyager 1* radio-occultation measurements. *Icarus* **53,** 348–363.

MOUNT, G. H., AND G. J. ROTTMAN 1981. The solar spectral irradiance 1200–3184 Å near solar maximum: July 15, 1981. *J. Geophys. Res.* **86,** 9193–9198.

NAVA, D. F., M. B. MITCHELL, AND L. J. STIEF 1986. The reaction H + C_4H_2: Absolute rate constant measurement and implication for atmospheric modeling of Titan. *J. Geophys. Res.* **91,** A4, 4585–4589.

SMITH, G. R., D. F. STROBEL, A. L. BROADFOOT, B. R. SANDEL, D. E. SHEMANSKY, AND J. B. HOLBERG 1982. Titan's upper atmosphere: Composition and temperature from the EUV solar occultation results. *J. Geophys. Res.* **87,** A3, 1351–1359.

SMITH, N. J. G., C. C. DAVID, AND I. W. M. SMITH 1985. Relaxation of C_2D_2 (ν_4,ν_5) by vibration–rotation, translation energy transfer. *J. Chem. Soc. Faraday Trans. 2* **81,** 417–432.

STEWART, A. I. 1972. Mariner 6 and 7 ultraviolet spectrometer experiment: Implications of CO_2^+, CO and O airglow. *J. Geophys. Res.* **77,** 54–68.

TORR, M. R., AND D. G. TORR 1985. Ionization frequencies for solar cycle 21: Revised. *J. Geophys. Res.* **90,** 6675–6678.

WANG, J. C. F., AND G. S. SPRINGER 1977. Vibrational relaxation times in CH_4–N_2 and C_2H_4–N_2 mixtures. *Prog. Astronaut. Aeronaut.* **51,** 849–858.

WEAST, R. C. 1981. *Handbook of Chemistry and Physics,* 62nd ed. CRC Press, Boca Raton.

YARDLEY, J. T., M. N. FERTIG, AND C. B. MOORE 1970. Vibrational deactivation in methane mixtures. *J. Chem. Phys.* **52,** 1450–1453.

YUAN, R. C. L., J. M. PRESES, G. W. FLYNN, AND A. M. RONN 1973. V-V and V-T/R energy transfer studies of C_2H_4 by infrared double resonance. *J. Chem. Phys.* **59,** 6128–6135.

YUNG, Y. L., M. ALLEN, AND J. P. PINTO 1984. Photochemistry of the atmosphere of Titan: Comparison between model and observations. *Astrophys. J. Suppl. Ser.* **55,** 465–506.